ELSEVIER

Journal of Molecular Catalysis A: Chemical 129 (1998) 249–256

JOURNAL OF MOLECULAR CATALYSIS A: CHEMICAL

Strong interaction between rhodium and ceria

Seiichiro Imamura [a,*], Tatsuro Yamashita [a], Rei Hamada [a], Yoshio Saito [a], Yukimichi Nakao [b], Noritoshi Tsuda [c], Chihiro Kaito [c]

[a] *Faculty of Engineering and Design, Kyoto Institute of Technology, Matsugasaki, Sakyo-ku, Kyoto 606, Japan*
[b] *National Institute of Materials and Chemical Research, Higashi 1-1, Tsukuba 305, Japan*
[c] *Faculty of Science and Engineering, Ritsumeikan University, 196 Noji-cho, Kusatsu, Shiga 525, Japan*

Received 25 March 1997; accepted 17 July 1997

Abstract

Rh was loaded on various supports including ceria by a colloid deposition method. The average particle size of the starting Rh colloid was about 50 Å. When it was deposited on alumina or zinc oxide, Rh particles were clearly observed by a TEM analysis. However, no TEM image of Rh was obtained on ceria which was prepared by calcination at 550°C. ESCA and XRD analyses revealed that Rh penetrated into the ceria and only a small amount remained on the surface. On the other hand Rh was present as metallic particles on the surface of ceria which was calcined at 950°C. The ceria calcined at a low temperature (550°C) had high surface area; thus, this ceria had high surface energy and could dissolve Rh. Although the amount of Rh exposed on the surface of ceria was small, the Rh in this state was highly active in decomposing methanol.

Keywords: State of rhodium; Ceria; TEM; ESCA; XRD; Methanol decomposition

1. Introduction

Ceria is an inevitable component in high performance automobile catalysts; it stabilizes support alumina and keeps surface area high [1,2], prevents the sintering of precious metals and thus stabilizes their dispersed state [3,4], promotes CO oxidation [5–7] and the water–gas shift reaction [8–10]. The most notable role of ceria is its oxygen-storage action, and many data are available concerning the migration of the lattice oxygen of ceria [11–20]. It is also used as a support for precious metals in reactions other than automobile exhaust gas detoxification, e.g., Pt-ceria for carbon monoxide hydrogenation [21], Rh-ceria for the decomposition of N_2O [22], and Ru-ceria for aqueous-phase or vapor-phase oxidation of formaldehyde [23,24]. As the superior action of ceria in these catalysts is often derived through the combination with precious metals, a knowledge of the interaction between ceria and precious metals is crucial to fully utilize the performance of both elements in designing efficient catalysts. However, there are discrepancies among the literature concerning whether precious metals aggregate on the surface of ceria or interact with it strongly so as to penetrate inside the bulk ceria. Cook et al. reported that sintering of Pt on alumina is retarded by an addition of ceria at

* Corresponding author. Fax: +81-75-7247534.

1381-1169/98/$19.00
PII S1381-1169(97)00183-0

600 and 800°C and assume the strong interaction of Pt with Ce; however, Pt particles were observed by TEM [3]. Zafiris and Gorte suggested the migration of Rh into ceria but without any clear evidence [20]. Brogan et al. reported the formation of a PtCeO complex on the basis of an analysis using Raman spectroscopy [25]. Kalakkad et al. observed the TEM image of Pt particles on any ceria supports used in the CO hydrogenation reaction [21]. Zhou et al. suggested the migration of Rh into ceria and the interaction of the former with Ce^{3+}. However, the extent of the interaction depends on the oxidation state of Ce: Rh retains its metallic state on the surface of a fully oxidized ceria [26]. Bernal et al. also investigated the interaction of ceria with Rh and obtained clear TEM images of Rh metal particles [27]. Thus the interaction of precious metals with ceria is complex and the results of the investigations differ among researchers. Previously we found that Rh supported ceria was very effective in decomposing nitrous oxide at low temperatures [22]. However, the state of Rh was not clarified. In this work colloidal Rh metal was prepared and was supported on ceria in order to regulate and fix the condition of the starting Rh, and the state of Rh was analyzed by the combined use of TEM, ESCA, and XRD techniques. Decomposition of methanol was carried out as a test reaction to evaluate catalyst performance.

2. Experimental

2.1. Catalyst preparation

Ammonia (3 M) was added to an aqueous solution of cerium(III) nitrate until the pH of the solution was 10. The resultant precipitate was washed three times with a sufficient amount of water and was dried at 80°C overnight, followed by calcination at 550°C in air for 3 h to give ceria (CeO_2) with a BET surface area of 58.8 m^2/g. Other supports (γ-Al_2O_3, ZnO, CaO, MgO, and ZrO_2) were used as obtained commercially.

Metallic rhodium was loaded onto the supports by a colloid adsorption method as follows [28]. Stable Rh hydrosol was obtained by adding 100 ml of an aqueous solution of $NaBH_4$ (40 mmol) to 2 l of water containing 20 mmol of $RhCl_3 3H_2O$ and polyethylene glycol-*p*-nonylphenyl ether (0.01 wt%). When the supports were dispersed into this solution and vigorously stirred, Rh hydrosol was completely adsorbed on their surface (1 wt%). The Rh-loaded supports were then calcined at 550°C in air for 3 h, followed by reduction in hydrogen at 300°C for 1 h.

2.2. Decomposition of methanol

Decomposition of methanol was carried out under an atmospheric pressure with an ordinary flow reactor. Catalysts were diluted with an inert ZrO_2 (calcined at 1300°C in air for 3 h) to 10 vol%, pressed into a disc under a pressure of 30 MPa, and were cut into 8–14 mesh size. Two ml of the catalyst was packed in the tubular reactor and was again reduced in hydrogen at 300°C for 30 min before reaction. Methanol (3.83 vol%) in Ar was fed into the reactor through a saturator maintained at 0°C at a space velocity of 21000 h^{-1}, and the temperature of the catalyst bed was increased at a rate of 2°C/min up to a maximum of 400°C.

2.3. Analyses

Methanol, formaldehyde, and dimethyl ether were determined with a Shimadzu 4B gas chromatograph on a Porapak T column (2 m) at 140°C. Methane, CO, CO_2, and H_2 were analyzed with a Shimadzu 3BT gas chromatograph on an activated charcoal column (1 m) at 60°C.

ESCA analysis was carried out by the use of a Shimadzu ESCA 750 spectrophotometer, and the bulk Rh content was determined with a Horiba EMAX-5770 energy dispersive x-ray spectrometer. TEM images were obtained with Hitachi H-9000 UHR and Hitachi H-7100 trans-

mission electron microscopes. The lattice constant of ceria was measured by an asymmetric photographic method using a Rigaku Denki Geigerflex D-3F equipped with a Debye-Scherrer camera. The radius of the camera was determined by the use of crystalline silicon powder as a standard. The 16 diffraction peaks of ceria observed by this method gave the averaged value of the lattice constant to a precision down to the third decimal place in Å unit.

3. Results and discussion

Fig. 1 shows a TEM micrograph of the Rh hydrosol as prepared. The average size of the hydrosol was about 50 Å, and several of these tended to be joined together. This hydrosol was loaded on the supports and calcined at 550°C in air, followed by reduction at 300°C in hydrogen. Figs. 2–4 show the TEM images of Rh-loaded ZnO, γ-Al_2O_3, and CeO_2, respectively. Aggregation of Rh primary particles (size ranging from 30–80 Å) occurred on ZnO to form large secondary particles. The (111) and (200) planes of Rh metal are clearly observed. Rh metal particles were also observed on γ-Al_2O_3. Thus Rh metal particles were omnipresent on these two supports as observed by the TEM technique. However, no Rh image was observed except that of CeO_2 (an average particle size of ca. 80 Å) as shown in Fig. 4, although the presence of Rh was clearly indicated by a spot analysis using an energy dispersive X-ray spectrophotometer (Rh: 0.619 atomic% = 1.1 wt% on CeO_2). Every effort to obtain HREM images of Rh failed, which suggests that Rh was too finely dispersed on the surface of CeO_2 to be observed by phase contrast or it had penetrated inside CeO_2 lattice.

Shown in Fig. 5 are the results of the decomposition of methanol to form CO and H_2. The

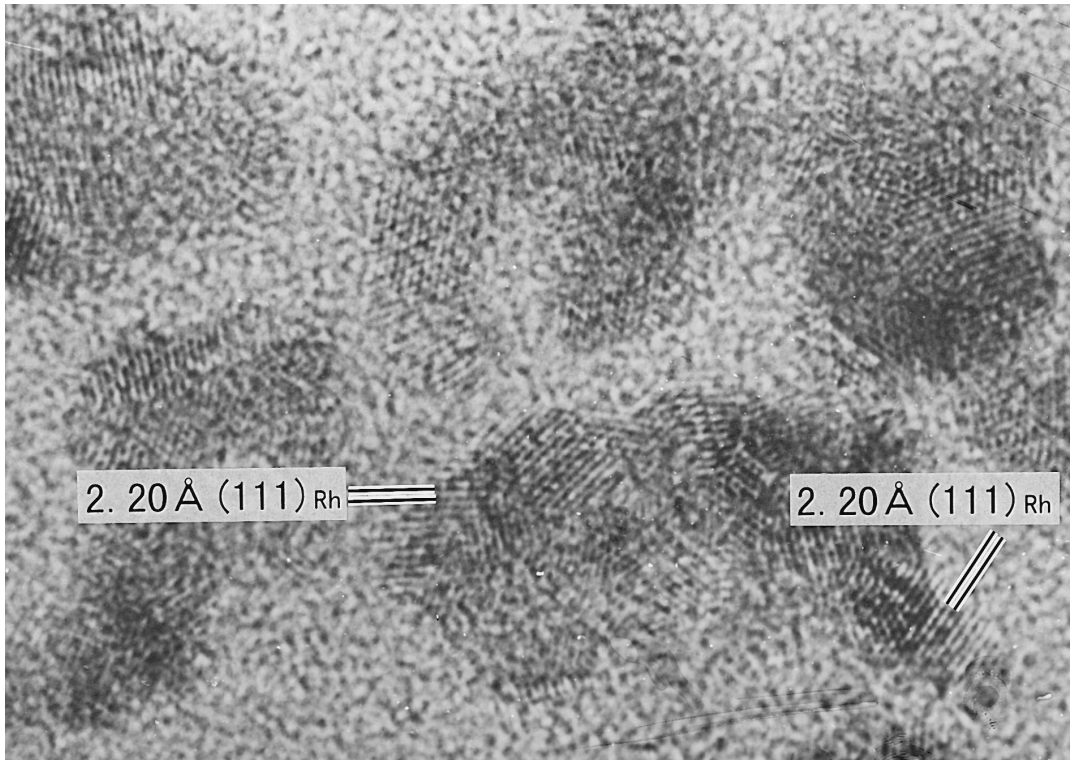

Fig. 1. TEM image of Rh colloid.

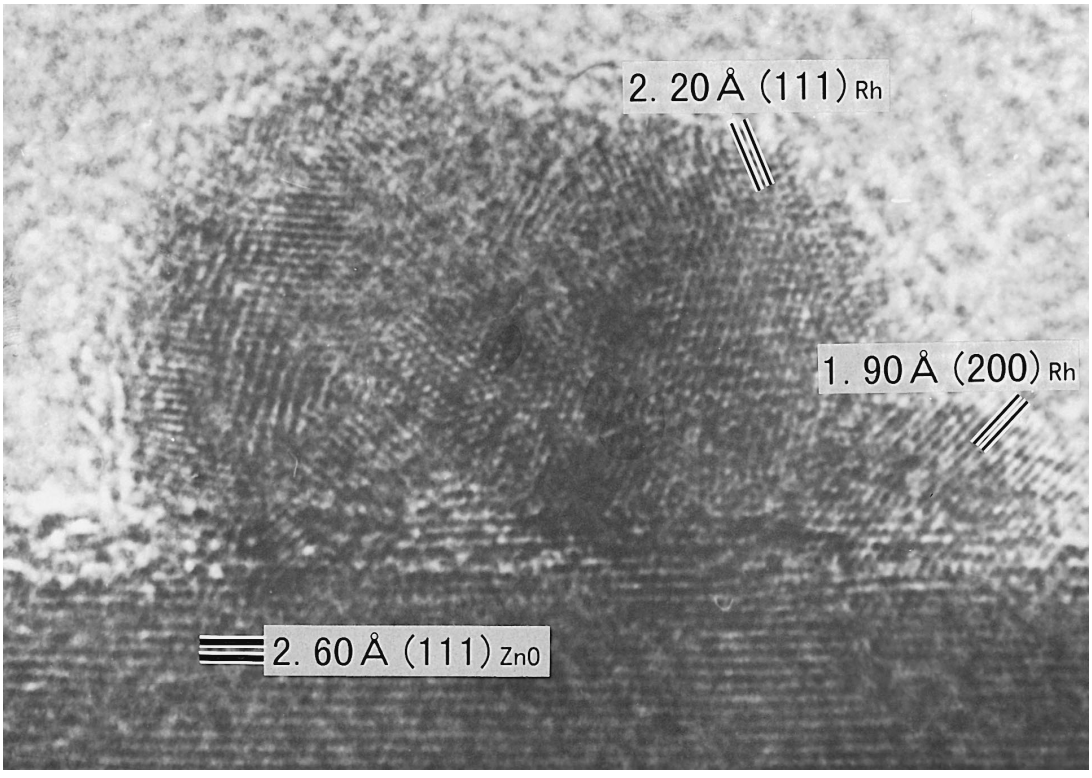

Fig. 2. TEM image of Rh/ZnO.

activity of Rh/CeO_2 is especially high, and there is not so much difference among the performance of the remaining catalysts. As the densities of the catalysts differed, the activity per unit amount of Rh may present a different performance order. However, Rh/CeO_2 was found to be the most active even by the evaluation based on unit Rh amount. BET surface areas (m^2/g) were 58.8 (CeO_2), 46.3(MgO), 169.2 (γ-Al_2O_3), 12.2 (ZrO_2), 19.6 (CaO), and 14.7 (ZnO). Thus the surface area of the support is not a limiting factor determining the catalyst activity. Table 1 shows the selectivity to the reaction products, hydrogen and carbon monoxide, at the temperature of 100% methanol conversion. The performance of Rh/CeO_2 is also the best; the selectivity to CO and H_2 is the highest at the lowest temperature (300°C). A small amount of formaldehyde was produced on Rh/CeO_2 and dimethyl ether was formed on all other catalysts. In particular, Rh/γ-Al_2O_3 formed a large amount of dimethyl ether in the low temperature region around 300°C. However, quantitative analysis of these two products was not carried out.

CeO_2 was found to be the best support for Rh for methanol decomposition. However, we could not clarify the state of Rh by the TEM technique. The fact that the HREM did not give the images of Rh suggests two possibilities as briefly addressed above. One is that Rh was so finely distributed on the surface of CeO_2 that it did not form a definite crystal structure that would give diffraction or mass contrast. The other possibility is that Rh penetrated inside the bulk of CeO_2. In order to study the latter possibility the change in the lattice constant of CeO_2 (a_0) on supporting Rh was monitored by an XRD analysis. In this case more than 1 wt% of Rh was supported on CeO_2, and this amount was too large for loading by the colloidal method. Thus Rh was supported as follows.

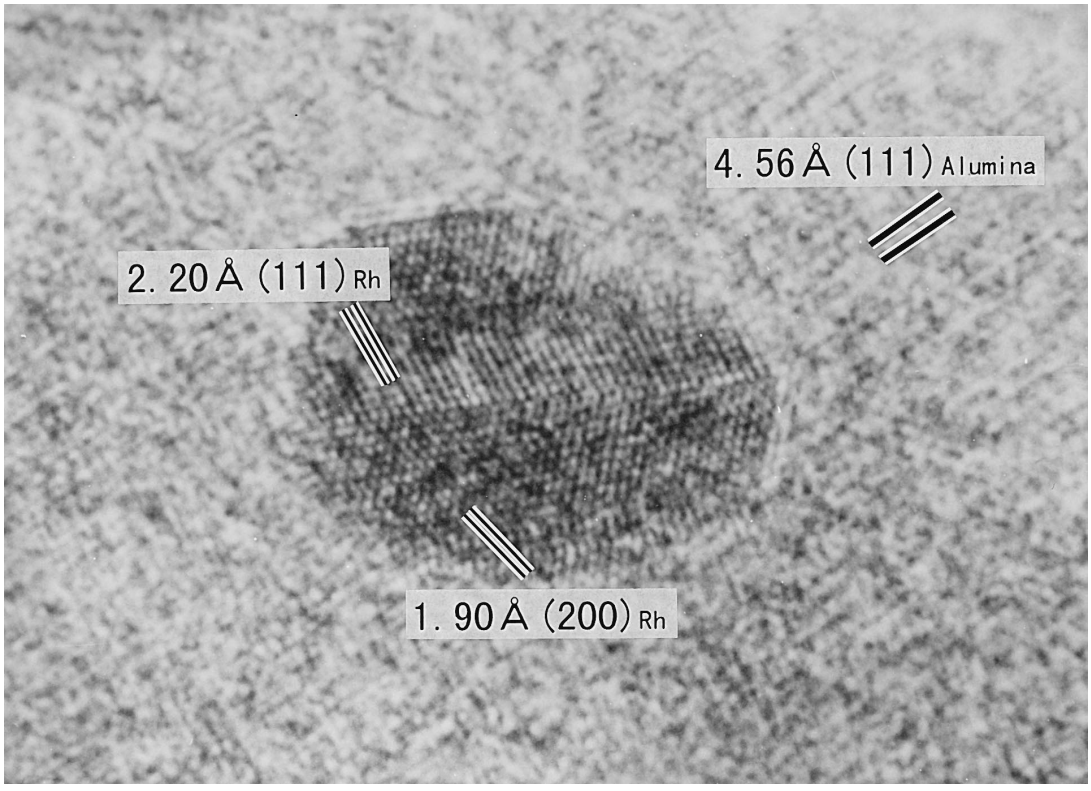

Fig. 3. TEM image of Rh/γ-Al_2O_3.

CeO_2 (5 g) was dispersed in 200 ml of an aqueous solution of rhodium(III) nitrate (known amounts) and the solution was kept at 70°C under stirring. Folmaldehyde (5 molar ratio to Rh) was added to the solution, which was kept stirring for 1 h. Then the mixture was evaporated and the residue was dried at 80°C overnight, followed by calcination at 550°C and subsequent reduction at 300°C as usual. CeO_2 calcined at 950°C in air had a value of a_0 of 5.412 Å which is in accord with the literature value for a stoichiometric CeO_2 cubic structure [29]. However, the a_0 of CeO_2, after calcination at 550°C and subsequent reduction at 300°C in the absence of Rh, was 5.414 ($\pm$0.002) Å. Thus this CeO_2 crystal is of a non-stoichiometric structure. On an addition of Rh the lattice constant further increased to 5.419 ($\pm$0.001) Å and 5.429 ($\pm$0.002) Å for 1 and 7 wt% of Rh, respectively. This result may indicate that the Rh penetrates inside the CeO_2 and enlarges its lattice parameter.

ESCA analysis was carried out to see the amount of Rh on the surface of CeO_2 (Fig. 6). The Rh/Ce molar ratio was calculated from the peak intensities of both elements (Rh: $3d_{3/2}$ plus $3d_{5/2}$, Ce: $4d_{3/2}$ plus $4d_{5/2}$) In this case the Rh was also supported on CeO_2 by the impregnation method as described above. With a Rh/Ce molar ratio of less than 0.052 (3 wt% of Rh loading), the surface molar ratio was almost the same as the ratio initially charged. On further addition of Rh, the surface Rh/Ce ratio began to exceed the charged ratio. However, even when the amount of Rh was increased to 5 wt% (Rh/Ce molar ratio of 0.088), the surface ratio increased only to 0.17. If the loaded Rh is present only on the surface, the Rh/Ce surface ratio should exceed the charged ratio by an order of magnitude. Shown also in

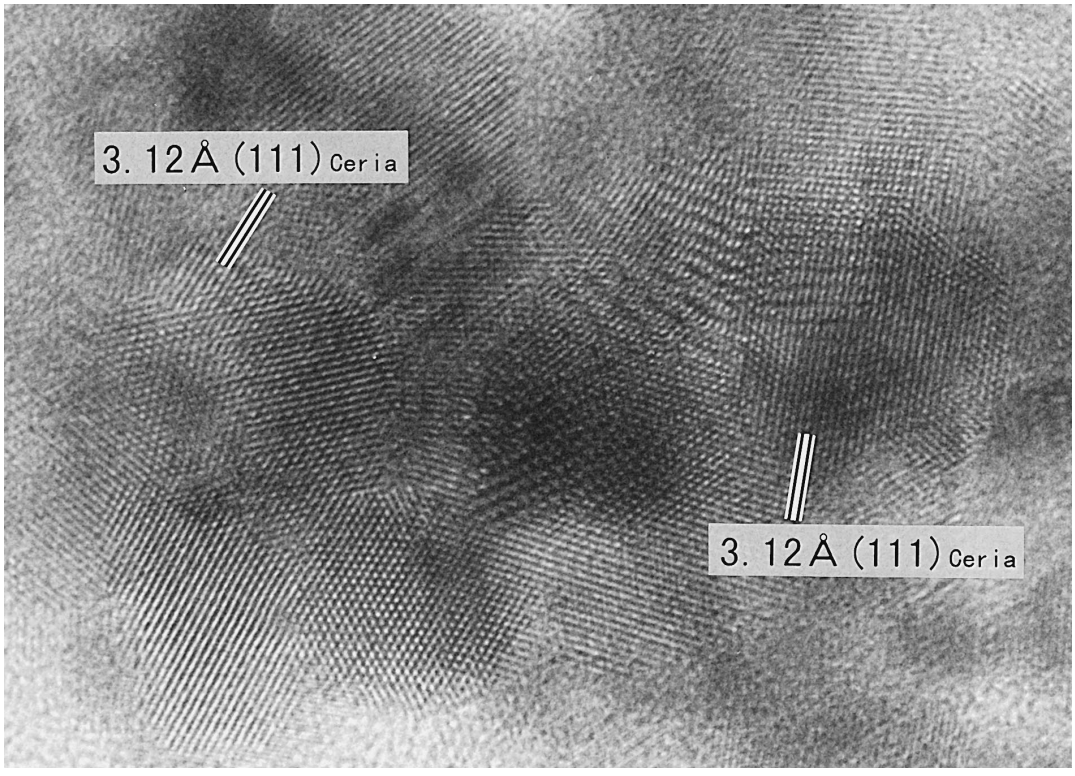

Fig. 4. TEM image of Rh/CeO_2. The CeO_2 was calcined at 550°C in air for 3 h.

Fig. 6 is the surface Rh/Ce ratio for the sample in which 1 wt% of Rh (Rh/Ce molar ratio of 0.017) was loaded on CeO_2 calcined at 950°C.

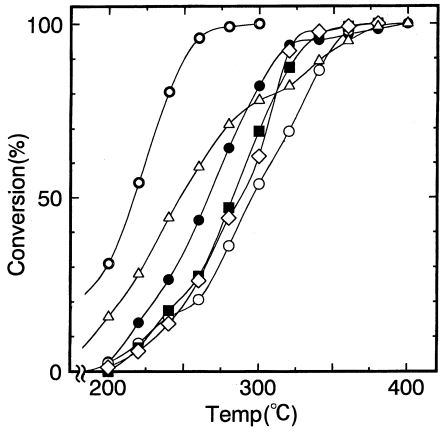

Fig. 5. Decomposition of methanol. (⊙) Rh/CeO_2, (△) Rh/ZrO_2, (●) Rh/γ-Al_2O_3, (■) Rh/MgO, (◇) Rh/ZnO, (○) Rh/CaO. Methanol: 3.83 vol% in Ar; catalyst: 2 ml diluted with inert ZrO_2 calcined at 1300°C to 10 vol%; space velocity: 21000 h^{-1}.

In this case surface Rh/Ce ratio was found to be much greater (0.49) compared with the charged value of 0.017.

A 0.2 wt% of Rh was supported on the CeO_2 calcined at 950°C by a colloid adsorption

Table 1
Decomposition of methanol[a]

Catalyst	Temp. (°C)[b]	Selectivity (%)[c]	
		CO	H_2
Rh/CeO_2	300	88.3	92.7
Rh/MgO	380	70.5	78.5
Rh/γ-Al_2O_3	400	73.1	82.0
Rh/ZrO_2	400	83.1	86.3
Rh/CaO	380	82.1	84.1
Rh/ZnO	380	43.7	77.7

[a] Methanol: 3.83 vol% in Ar; catalyst: 2 ml diluted with inert ZrO_2 calcined at 1300°C to 10 vol%; space velocity: 21000 h^{-1}.
[b] Complete conversion of methanol was first attained at this temperature.
[c] A small amount of formaldehyde was produced on Rh/CeO_2, and dimethyl ether on other catalysts. Rh/γ-Al_2O_3 formed a large amount of dimethyl ether at around 300°C.

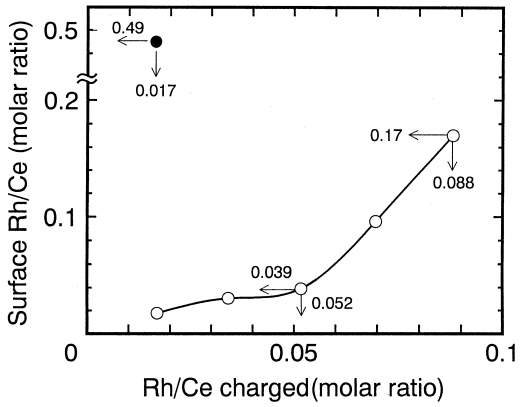

Fig. 6. ESCA analyses of surface Rh/Ce vs. charged Rh/Ce. (○): CeO_2 calcined at 550 °C, (●) CeO_2 calcined at 950°C.

method; 0.2 wt% was the maximum quantity of Rh to be loaded by this method because the surface area of the CeO_2 was low as described below. After this Rh-loaded CeO_2 was treated in air and hydrogen as usual, its TEM image was obtained (Fig. 7). Rh metal particles are clearly seen on the surface of a large particle-size CeO_2. The presence of Rh in the region of CeO_2 shown in the photograph was also confirmed with the energy dispersive X-ray spectrometer. As the CeO_2 was calcined at a high temperature (950°C), extensive crystal growth occurred, as shown in the TEM image, and thus its BET surface area was only 0.76 m^2/g.

The results obtained so far give a knowledge concerning the behavior of Rh on CeO_2. The CeO_2 calcined at low temperature (550°C) has a large surface area (58.8 m^2/g), and, thus, seems to have a high surface energy. Therefore, it interacts with Rh so strongly as to dissolve Rh easily inside the bulk as is shown by the small surface Rh content (ESCA result shown in Fig. 6). On the other hand, as the surface area of the CeO_2 calcined at a high temperature (950°C) is very small (0.76 m^2/g) and its surface activity is low, dissolution of Rh is difficult. Bernal et al. reported that Rh metal particles (similar to but much smaller than those shown in Fig. 7) were observed with a TEM on CeO_2 with a relatively small surface area (7 m^2/g) after a reduction with hydrogen at 350°C [27]. However, a clear TEM image of Rh could not be obtained on a large surface area CeO_2 (130 m^2/g) unless the reduction temperature was increased to 500°C. Thus the extent of the interaction between Rh and Ce seems to depend on the activity of the surface of CeO_2. However, surface area is not the only factor to affect the dissolution of Rh because γ-Al_2O_3 has much larger surface area (169.2 m^2/g) than CeO_2 but has no ability to incorporate Rh inside its bulk (Fig. 2). Thus CeO_2 has a peculiar interaction with Rh which is different from other supports, and this interaction could be one of the causes for its high catalytic performance when combined with precious metals as in automobile catalyst and other catalyst systems. It is interesting to note that Rh/CeO_2 exhibits high activity in the decomposition of methanol or in the decomposition of N_2O [22] even though most of the Rh is hidden inside the CeO_2 and only a small portion participates in the reaction.

Although some information on the behavior of Rh on CeO_2 was obtained, the state of Rh could not be clarified. EXAFS analysis of the Rh failed due to the strong background absorption of Ce. The binding energy of the ESCA $3d_{5/2}$ peak of Rh in 1 wt% Rh/CeO_2 (prepared by the colloid absorption method) was 308.8 eV, which is similar to the literature value of 308.7 eV for Rh_2O_3 [30]. This may indicate that

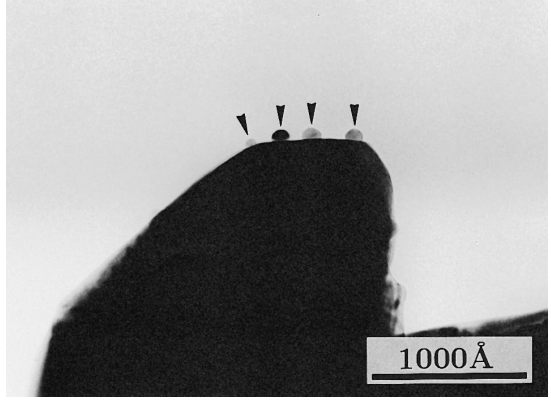

Fig. 7. TEM image of Rh/CeO_2. The CeO_2 was calcined at 950°C in air for 3 h.

Rh interacts with CeO_2 in the form of some kind of composite oxides. However, details are not known now and need further clarification.

Acknowledgements

This research was supported by a Grant-in-Aid for Scientific Research Project on Catalytic Chemistry of Unique Reaction Fields-Extreme Environment Catalysis (No. 08232101). The authors thank Dr. Y. Matsumura of Osaka National Research Institute and Dr. H. Kanai of Kyoto Prefectural University for their useful suggestion and cooperation. They also acknowledge the cooperation of Mr. K. Utani of Kyoto Institute of Technology.

References

[1] B. Harrison, A.F. Diwell, C. Hallett, Plat. Met. Rev. 32 (1988) 73.
[2] M. Ozawa, M. Kimura, J. Mater. Sci. Lett. 9 (1990) 291.
[3] A. Cook, A.G. Fitzgerald, J.A. Cairns, in: T.J. Dines, C.H. Rochester, J. Thomson (Eds.), Catalysis and Surface Characterization, Royal Society of Chemistry, Cambridge, 1992, p. 249.
[4] F.L. Normand, L. Hilaire, K. Kili, G. Maire, J. Phys. Chem. 92 (1988) 2561.
[5] Y.F.Yu. Yao, J. Catal. 87 (1984) 152.
[6] J.G. Numan, H.J. Robota, M.J. Cohn, S.A. Bradley, J. Catal. 133 (1992) 309.
[7] C. Serre, F. Garin, G. Belot, G. Maire, J. Catal 141 (1993) 1.
[8] J.C. Schlatter, P.J. Mitchell, Ind. Eng. Chem. Prod. Res. Dev. 19 (1980) 288.
[9] G. Kim, Ind. Eng. Chem. Prod. Res. Dev. 21 (1982) 267.
[10] E.C. Su, W.G. Rothschild, J. Catal. 99 (1986) 506.
[11] S. Imamura, M. Shono, N. Okamoto, A. Hamada, S. Ishida, App. Catal. A. 142 (1996) 279.
[12] H.C. Yao, Y.F. Yu Yao, J. Catal. 86 (1984) 254.
[13] E.C. Su, C.N. Montreuil, W.W. Rothschild, Appl. Catal. 17 (1985) 75.
[14] B.H. Engler, E. Koberstein, P. Schubert, Appl. Catal. 48 (1989) 71.
[15] P. Loof, B. Kasemo, K.E. Keck, J. Catal. 118 (1989) 339.
[16] T. Miki, T. Ogawa, M. Haneda, N. Kakuta, A. Ueno, S. Tateishi, S. Matsuura, M. Sato, J. Phys. Chem. 94 (1990) 339.
[17] C. Padeste, N.W. Cant, D.L. Trimm, Catal. Lett. 18 (1993) 305.
[18] S. Kacimi, J. Barbier Jr., R. Taha, D. Duprez, Catal. Lett. 22 (1993) 343.
[19] G.S. Zafiris, R.J. Gorte, J. Catal. 143 (1993) 86.
[20] G.S. Zafiris, R.J. Gorte, J. Catal. 139 (1993) 561.
[21] D.S. Kalakkad, A.K. Datye, H.J. Robota, J. Catal. 148 (1994) 729.
[22] S. Imamura, N. Okamoto, Y. Saito, T. Ito, H. Jindai, J. Jpn. Petrol. Inst. 39 (1996) 350.
[23] S. Imamura, I. Fukuda, S. Ishida, Ind. Eng. Chem. Res. 27 (1988) 718.
[24] S. Imamura, D. Uchihori, K. Utani, T. Ito, Catal. Lett. 24 (1994) 377.
[25] M.S. Brogan, J.A. Cairns, T.J. Dines, in: T.J. Dines, C.H. Rochester, J. Thomson (Eds.), Catalysis and Surface Characterization, Royal Society of Chemistry, Cambridge, 1992, p. 282.
[26] T. Zhou, M. Nakashima, J.M. White, J. Phys. Chem. 92 (1988) 812.
[27] S. Bernal, F.J. Botana, J.J. Calvino, M.A. Cauqui, G.A. Cifredo, A. Jobacho, J.M. Pintado, J.M. Rodiguez-Izquierdo, J. Phys. Chem. 97 (1993) 4118.
[28] Y. Nakao, K. Kaeriyama, Chem. Lett. (1993) 949.
[29] J.V. Smith (Ed.), in: X-Ray Powder Data File, Sets 1–5, American Society for Testing and Materials, Pennsylvania, 1967, p. 534.
[30] D. Briggs, M.P. Seah (Eds.), in: Practical Surface Analysis, 2nd Ed., Vol. 1 — Auger and X-ray Photoelectron Spectroscopy, Wiley, New York, NY, 1990, p. 613.